IEE Swansea Conference Sept. 1991 ADC/DAC.

BANDPASS IMPLEMENTATION OF THE SIGMA-DELTA A-D CONVERSION TECHNIQUE

A.M. Thurston, T.H. Pearce and M.J. Hawksford*

GEC-Marconi Research Centre, UK.
* University of Essex, UK.

INTRODUCTION

The technique of base-band sigma-delta Analogue to Digital (A-D) conversion is well established where in 1962 the formal structure of 2-level quantisation in association with a noise shaping, analogue feedback loop was presented for speech and communication applications [1, 2]. More recently, single-bit conversion schemes have found a wider application in digital-audio systems for both A-D converters and Digital to Analogue (D-A) converters where enhanced linearity especially at low signal levels is a principal advantage.

For RF applications the base-band conversion scheme requires demodulation of the message using two matched mixers fed by inphase and quadrature carriers. The output of each mixer is then low pass filtered and subsequently encoded with separate A-D converters. While this approach may be satisfactory for low resolution systems it has inherent performance limitations due to I-Q imbalance and sensitivity at the carrier due to masking by dc offsets.

A new design of band-pass sigma-delta A-D converter is presented which can encode the signal at the intermediate frequency and then by digital post processing convert to baseband I and Q. The technique of band-pass sigma-delta conversion is described and a method for designing band-pass A-D converters from existing baseband modulator designs is given with an example to illustrate the theory. Practical results are described with the performance specified in conventional RF circuit terms.

BASEBAND SIGMA DELTA MODULATION

A number of baseband modulator architectures have been published since 1962, examples of which are described in Refs 3-8. The noise shaping properties of the modulator are defined by the transfer function around the loop, by the number of quantising levels in the quantiser and by the nature of the input signal. Many of the published architectures have identical noise shaping properties, and a baseband modulator typical of these is selected for conversion to bandpass implementation, Figure 1. The term "modulator" is used here to describe a sampled data implementation of a sigma delta loop, whereas the term "converter" implies an architecture with D-A converters, analogue filters and a comparator.

Modelling the quantiser as a unity gain buffer with an added noise source gives a noise shaping function of

$$NSF_1(z) = \frac{(z-1)^2}{z^2} \qquad \ldots(1)$$

which has a double pole at the origin and a double zero at z=1. Noise is hence suppressed at low frequencies.

CONVERSION TO BANDPASS

The modulator may easily be converted to allow suppression of the quantising noise at other frequencies by simple substitutions for z. The most straight forward of these is to substitute -z for z. The noise shaping function for such a modulator would be given by

$$NSF_2(z) = \frac{(z+1)^2}{z^2} \qquad \ldots(2)$$

and would have a double pole at the origin and a double zero at z=-1. It would therefore suppress noise around half the sampling frequency. However this modulator would be of little practical use since aliasing would prevent discrimination of components above or below the half sampling frequency.

To avoid problems caused by aliasing a better substitution is that of $-z^2$ for z, giving the modulator shown in Figure 2. The noise shaping function for this modulator is given by

$$NSF_3(z) = \frac{(z^2+1)^2}{z^4} \qquad \ldots(3)$$

and has a double zero at both z=j and z=-j and a quadruple pole at the origin. Noise in this modulator is suppressed at the one quarter and three quarters sampling frequency and it may therefore be used to modulate signals close to either of these without aliasing [9].

IMPULSE INVARIANT DESIGN

The conversion of digital modulators into converters of mixed analogue and digital construction is based upon the impulse invariant design technique. The objective is to design an analogue filter for which the sampled response to a pulse from the D-A converter is identical to the impulse response of the loop filter in the digital modulator. This is illustrated in Figure 3, and is expressed mathematically by

$$\mathcal{Z}^{-1}H(z) = \mathcal{L}^{-1}G(s).DAC(s) \qquad t=nT \qquad \ldots(4)$$

where H(z) is the z transform of the digital loop filter, G(s) is the Laplace transform of the required analogue loop filter, and DAC(s) is the Laplace transform of one output pulse of the D-A converter. No direct general solution exists for equation (4) and so it must be solved by an analytic means for each case.

BANDPASS CONVERTER ARCHITECTURE

The design of the A-D converter requires both that the analogue IF input signal is summed with the output of a D-A converter prior to bandpass filtering and that the response of the bandpass filter to a pulse from the D-A converter, or converters, is the impulse invariant equivalent of the loop filter shown in Figure 2. Figure 4 shows the architecture of such an A-D converter. At the resonant frequency the filter has no phase shift whereas the delay in the feedback path introduces a 180 degree phase shift. For this reason the signal is added to rather than subtracted from the input signal at the summing node.

CONVERTER DESIGN

Impulse Response Of Digital Loop Filter

The loop filter required to produce the noise shaping function given in (3) is given by

$$H(z) = \frac{2z^4 + z^2}{(z^2+1)^2} \qquad \ldots(5)$$

Its impulse response is found by taking the inverse z transform and is given by

$$h(n) = \mathcal{Z}^{-1} H(z) \qquad \ldots(6)$$

$$= \left(2 + \frac{n}{2}\right)\cos\left(\frac{\pi n}{2}\right) \qquad n = 0, 1, 2 \ldots \quad \ldots(7)$$

For a sampling rate of $f_s = 1/T$ this may be written as

$$h(t) = \left(2 + \frac{t}{2T}\right)\cos\left(\frac{\pi t}{2T}\right) \qquad t = nT \qquad \ldots(8)$$

For solution of the analogue filter this may now be equated to the RHS of equation (4) giving

$$\mathcal{L}^{-1} G(s).DAC(s) = \left(2 + \frac{t}{2T}\right)\cos\left(\frac{\pi t}{2T}\right) \qquad t = nT \quad \ldots(9)$$

D-A Converters

The output of each of the D-A converters is a current pulse of a polarity matching that of the data. Each pulse has a duration $T = 1/f_s$ and for the purpose of analysis is deemed to be centred on $t = 0$. The magnitude of the current pulses are $\pm I_1$, $\pm I_2$ and $\pm I_3$, for the first, second and third D-A converters respectively. The Laplace transform of the output of each D-A converter is given by

$$DAC_m(s) = I_m\left[\frac{e^{\frac{sT}{2}} - e^{-\frac{sT}{2}}}{s}\right] \qquad m = 1, 2, 3. \quad \ldots(10)$$

Analogue Loop Filter

The loop filters are modelled as lossless since this considerably simplifies the mathematics and has little effect on the solved component values. The loop filters are tuned to one quarter of the sampling frequency.

$$\omega_n = \frac{1}{\sqrt{LC}} = \frac{\pi f_s}{2} \qquad \ldots(11)$$

The first and second buffer amplifiers have transconductances of K_1 and K_2 respectively.

Solution By Impulse Invariant Method

The Laplace transform of the response of the analogue filter to simultaneous pulses from the D-A converters is given by

$$G(s).DAC(s) = \left[I_1K_1K_2\left(\frac{1}{C}\cdot\frac{s}{s^2+\omega_n^2}\right)^2 + I_2K_2\left(\frac{1}{C}\cdot\frac{s}{s^2+\omega_n^2}\right) + I_3\right].R.\left[\frac{e^{\frac{sT}{2}} - e^{-\frac{sT}{2}}}{s}\right] \quad \ldots(12)$$

This may now be used in (9) to give

$$\mathcal{L}^{-1}\left[I_1K_1K_2\left(\frac{1}{C}\cdot\frac{s}{s^2+\omega_n^2}\right)^2 + I_2K_2\left(\frac{1}{C}\cdot\frac{s}{s^2+\omega_n^2}\right) + I_3\right].$$
$$R.\left[\frac{e^{sT/2} - e^{-sT/2}}{s}\right] = \left(2 + \frac{t}{2T}\right)\cos\left(\frac{\pi t}{2T}\right) \quad | t = nT \qquad \ldots(13)$$

Analysis of the LHS of (13) must be split into two regions, $-T/2 \leq t < T/2$ for solution when $n = 0$, and $t \geq T/2$ for solution $n > 0$.

In the first region, the LHS of (13) is given by

$$\left[\frac{I_1K_1K_2}{2\omega_nC^2}\left(t + \frac{T}{2}\right)\sin\left(\omega_nt + \frac{\pi}{4}\right) + \frac{I_2K_2}{\omega_nC}\sin\left(\omega_nt + \frac{\pi}{4}\right) + I_3\right].R \quad -\frac{T}{2} \leq t < \frac{T}{2} \qquad \ldots(14)$$

which must be equated to 2 units of voltage at $t = 0$.

For subsequent values of n, the LHS of (13) is given by

$$\left[\frac{I_1K_1K_2}{2\omega_nC^2}\left(T\cos\left(\frac{\pi}{4}\right)\sin(\omega_nt) + 2t\sin\left(\frac{\pi}{4}\right)\cos(\omega_nt)\right)\right.$$
$$\left. + \frac{2I_2K_2}{\omega_nC}\left(\sin\left(\frac{\pi}{4}\right)\cos(\omega_nt)\right)\right].R \quad t \geq \frac{T}{2} \qquad \ldots(15)$$

This is equated to the RHS of (9) for n=1, 2, 3 ... The residual term in $\sin \omega_n t$ found in (15) is sufficiently small as to be ignored, a conclusion confirmed by practical results.

PRACTICAL IMPLEMENTATION

A typical set of results produced with equations (9), (14) and (15) for an A-D converter sampling at 10 MHz and encoding an IF signal centred at 2.5 MHz is given in Table 1.

Table 1 Practical Circuit Parameters

f_s	10.0MHz
C	1000pF
L	4.05μH
R	1 kΩ
K_1	10 mS
K_2	10 mS
I_1	1.111mA
I_2	2.221mA
I_3	0.875mA

PERFORMANCE

Figure 5a shows the spectrum of the single bit data output of a converter implemented in the manner of Figure 4 at a sample rate of 10 MHz. The display shows a well defined notch around 2.5 MHz together with the in-band signal. Figure 5b shows the performance across the 100 kHz converter passband at the centre of the notch. The results for this were taken after digital quadrature mixing to I and Q signals at baseband followed by decimating low pass filters as shown in Figure 6. Blocks of 1024 samples are stored from the decimation filter output and then transferred to a desk top computer (PC) for FFT analysis [10]. The left-hand vertical scale represents the level in dB below the converter overload point and the right-hand scale the corresponding absolute level in dBm. The frequency scale covers the 100 kHz converter passband centred on the 2.5 MHz IF at the converter input. The equivalent noise bandwidth is 200 Hz in each FFT analysis bin after taking account of windowing.

Peak Signal to Noise Ratio

The quantisation noise density across the 100 kHz passband is found to be 94 dB below the converter overload point in 200 Hz, equivalent to 117 dB in 1 Hz bandwidth.

The signal to quantisation noise density for a sine wave just filling the range of a uniform quantiser of n bits, sampled at rate f_s and assuming the quantisation noise power to be uniformly distributed across the half sampling frequency passband, is given by

$$S/N(1Hz) = 6.02n + 1.76 + 10\log\left(\frac{f_s}{2}\right) \; dB \quad ...(16)$$

Using this equation it is found that an ideal 8 bit quantiser sampling at 10 MHz would give a peak signal to noise density of 117 dB in 1 Hz. Thus within the 100 kHz passband of the sigma-delta converter the resolution is equivalent to an 8 bit conventional converter sampling at 10 MHz, but with the information being carried by a single bit. After mixing to baseband I and Q signals and low pass filtering as shown in Figure 6, the sample rate can be reduced to a value commensurate with the converter passband. The signal at this stage is then multi-bit and equivalent to a resolution of 11 bits at 100 kHz sample rate on I and Q.

I,Q Orthogonality

The use of digital I,Q mixing to baseband avoids the I,Q imbalance and carrier frequency sensitivity limitations found with more conventional analogue quadrature mixing followed by separate baseband A-D converters for I and Q. It is seen from Figure 5b that I,Q images are at least 80 dB below the tone level and similarly no component appears at the carrier frequency, which would result from DC offsets in the analogue I,Q mixing arrangement.

Linearity

A particular feature of the converter compared with more conventional successive approximation or flash A-D converters is the closer approximation in the behaviour of intermodulation products with signal level to a purely analogue circuit. Figure 7 shows a plot of third order intermodulation product level variation with signal level where it is seen that the products follow an approximate three dB per dB relationship. This is in contrast to the behaviour of flash converters in particular, where the intermodulation products tend to remain almost independent of signal level, at typically only 55 to 60 dB below overload for an 8 bit device, shown by the shaded region in Figure 7, [10].

The third order intercept point (IP_3) is indicated on Figure 7 and calculated from the values of tone and intermodulation product level (IMP) as:

$$IP_3 = ToneLevel + \frac{1}{2}[ToneLevel - IMP] \quad ...(17)$$

From Figure 5b the overload point of the converter is seen to be -10 dBm while the third order intermodulation products (IMP) are 80 dB below the tone level of -24 dBm, giving a third order intercept point of:

$$IP_3 = -24 + \frac{80}{2} = +16 \; dBm$$

Using this well behaved linearity characteristic it becomes more appropriate to specify the performance in conventional RF circuit terms, i.e. a noise figure and third order intercept point, giving a spurious free dynamic range, an overload point analogous to the 1 dB compression point and a usable bandwidth.

Spurious Free Dynamic Range

The two tone spurious free dynamic range is defined as the difference between the tone and intermodulation product level where the tone level is such that the intermodulation products just equal the noise in a specified resolution bandwidth B. This is usually expressed in terms of the intercept point and noise figure, given for third order non-linearity by:

$$SFDR = \frac{2}{3}[IP_3 - (N_0 + NF + 10\log B)] \; dB \quad ...(18)$$

where IP_3 - Third order intercept dBm

N_0 - Thermal Noise Power Density

= -174 dBm (1 Hz)

NF = Noise Figure dB.

The Noise Figure is given by

NF = overload point $-S/N - N_0$

= -10 -117 +174

= 47 dB

Using a third order intercept point of +16 dBm, the spurious free dynamic range in 1 Hz bandwidth using eqn (18) then becomes

SFDR = 2/3 {16+174-47} = 95.3 dB(1 Hz)

CONCLUSIONS

The paper has described the development of a bandpass sigma-delta A-D converter design from a conventional baseband sigma-delta converter structure. The bandpass converter enables the conversion of band limited IF signals to baseband I and Q format with a high degree of I,Q orthogonality and full sensitivity at the IF centre frequency. Practical results for a converter designed to operate on an IF of 2.5 MHz demonstrate a spurious free dynamic range of 95 dB (1 Hz) across a passband of 100 kHz. The well behaved third order linearity yields a converter more closely approximating the characteristics of a purely analogue circuit, than conventional flash and successive approximation converters. These features make the converter particularly well suited to receiver IF processing. Also the converter is well suited to specification by the familiar RF parameters of noise figure, third order intercept point, overload and bandwidth, making the specification of parameters such as quantisation accuracy in bits resolution and integral and differential non-linearity no longer appropriate.

REFERENCES

[1] Inose H. Yasuda Y. and Murakami J., "A Telemetering System by Code Modulation - Sigma Delta Modulation", IRE Trans. Space Elect. and Telemetry, pp. 204-209, September 1962.

[2] Spang H.A. and Schulteiss P.M., "Reduction of Quantising Noise by Use of Feedback", IRE Trans Commun. Syst., pp 373-380, December 1962.

[3] Candy J.C., "A Use of Double Integration in Sigma Delta Modulation", IEEE Trans. Commun., Vol. COM-33, pp249-258, March 1985.

[4] Tewksbury S.K., and Hallock R.W., "Oversampled, Linear Predictive and Noise-Shaping Coders of Order N>1", IEE Trans Circuits Syst., Vol. CAS-25, pp. 436-442, July 1978.

[5] Boser B.E. and Wooley B.A., "The Design of Sigma-Delta Modulation Analog-to-Digital Converters", IEEE J. Solid-State Circuits, Vol. 23, pp. 1298-1308, December 1988.

[6] Agrawal B.P. and Shenoi K., "Design Methodology for ΣΔM", IEEE Trans. Commun., Vol. COM-31, pp. 360-370, March 1983.

[7] Hawksford M.J., "Nth-Order Recursive Sigma-ADC Machinery at the Analogue-Digital Gateway", AES 78th Convention, Anaheim, May 3-6 1985, Preprint 2248 A-15.

[8] Ichimura K., Hayashi T., Kimura T. and Iwati A., "Oversampling A-to-D and D-to-A Converters with Multistage Noise Shaping Modulators", IEEE Trans. Acoustics, Speech and Sig. Proc., Vol. 36, No. 12, pp. 1899-1905, December 1988.

[9] Pearce T.H. and Baker A.C., "Analogue to Digital Conversion Requirements for HF Radio Receivers", IEE Colloquium on "Systems Aspects and Applications of ADC's for Radar, Sonar and Communications", November 1987, Digest No. 1987/92.

[10] Pearce T.H. and Jay M.J., "Performance Assessment for Digitally Implemented Radio Receivers", IEE Conference on Radio Receivers and Associated Systems, Cambridge, July 1990, Conference Publication No. 325, pp. 113-117.

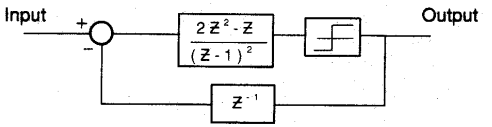

Fig 1. Baseband $\Sigma\Delta$ modulator

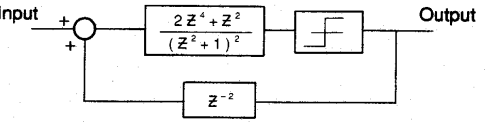

Fig 2. Bandpass $\Sigma\Delta$ modulator

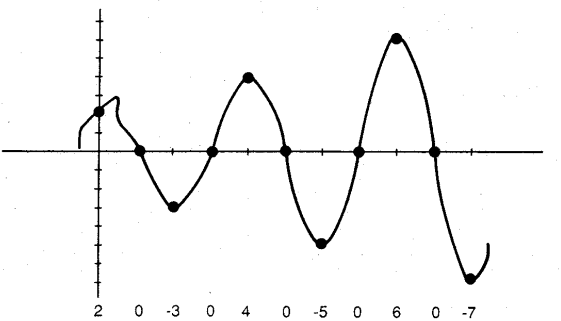

Fig 3. Impulse response demonstrating the impulse invariant transformation

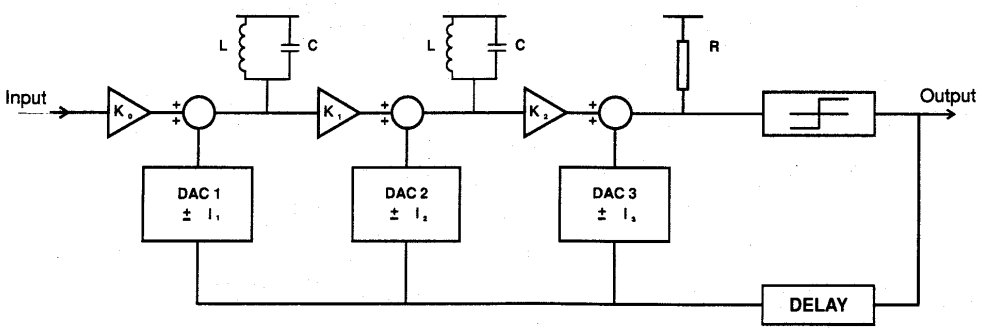

Fig 4. Bandpass $\Sigma\Delta$ converter structure

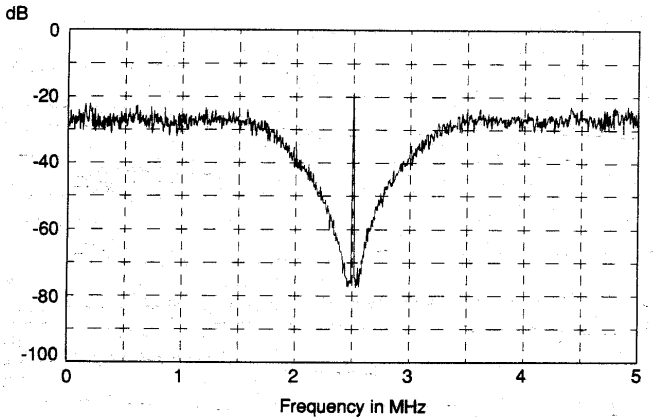

(a) Out of band

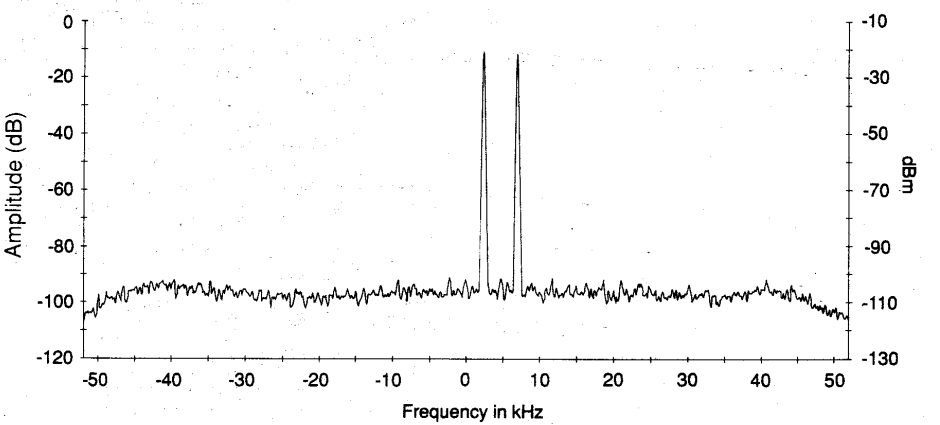

(b) In band

Fig 5. Frequency domain performance

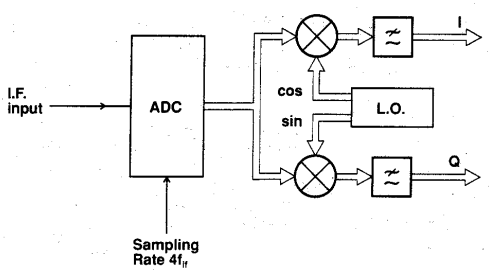

Fig 6. Post A-D converter processing

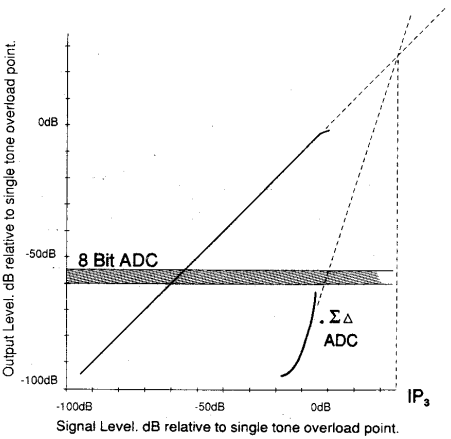

Fig 7. Linearity performance